Exploitation of Hertz's contact pressures in friction drives

D. Herák[1], R. Chotěborský[2], A. Sedláček[1], E. Janča[1]

[1]Department of Mechanics and Engineering, Technical Faculty, Czech University
of Agriculture in Prague, Prague, Czech Republic
[2]Department of Material and Engineering Technologies, Technical Faculty,
Czech University of Agriculture in Prague, Prague, Czech Republic

Abstract: The paper is intent on the applications of equations which describe the Hertz's surface pressures in friction drives. In the paper the reduced equations are derived, which are useful to the surface pressures calculation in friction drives when ball – ball, cylinder – cylinder, cone – cone are kept in touch and their graphical representation of stress distribution in the contact area is presented. Using the Hertz's surface pressures and the Mohr's circles the substance of pitting start is derived and the stress distributions using the elementary joists, which were situated on the axe z in the section under the contact joist, are represented.

Keywords: contact pressures; friction drive; Hertz's pressures; pitting; friction force; Mohr's circles

At friction drives the circumference power is transmitted by friction from one rolling body to the second. Always the thrust is necessary. At most designs of friction drives it deduces high forces to shafts and bearings. Therefore the high surface pressures result on the contact joists. These pressures are one of main factors which influence the friction drives.

The basic condition of friction drive is based on the equilibrium of circumference power F_0 and friction power F_t. When we speculate about the degree of safety k (starting, turning-out, impact influences etc.) we get the basic condition in the form

$$F_0 \times k = F_t \tag{1}$$

When we express the friction power as the product of the thrust F_K and coefficient of friction f and introduce it in the foregoing equation we get the basic condition of the friction drive (Figure 1).

$$F_0 \times k = f \times F_n \tag{2}$$

According to the contact we can classify the surface pressures as the surface contact, line contact, point contact.

According to the material elasticity we can classify the surface pressures in:

Hertz's pressures – the modulus of elasticity in tension of both materials is constant, owing to load it does not vary.

Stribeck's pressures – the modulus of elasticity in tension of one of materials is not constant, it varies according to the load (rubber, plastic etc.).

In friction drives operation the Hertz's pressures are in foreground and they influence considerably the drive, namely pressures with line and point contact.
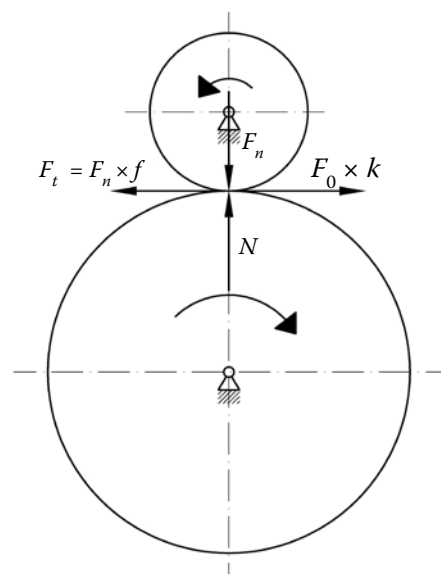
Therefore this paper is intent on these pressures.

Figure 1. Functional diagram of the friction drive

Hertz's surface pressures

As early as in the year 1881 Heinrich Hertz formulated the relation between the load value of projected area of surface pressures and the bringing near at the contact of generally curved bodies. The solution derived by Heinrich Hertz gives only the orientation values of contact pressures. The in this way calculated contact pressures can very in some cases as much as 50% from real values (Klaprodt 1980). Later much authors tried to describe the contact pressures theory. But till now the accurate solution of the contact pressures calculation was not found. (Klaprodt 1980; Bolek & Kochman 1990).

Heinrich Hertz introduced several simplified premises.

The place of the highest stress is under the middle of the upper surface of function of both bodies and near the front surface is the accumulation of stress.

The modulus of elasticity in tension of both materials is constant, it does not vary according to the load. Strains are regarding to the bodies sizes very low and their profile is in one plane (Hertz 1896).

For the calculation these four laws defined by Heinrich Hertz are valid.

(1) Isotropy and homogenity of projected area material.
(2) In the course of deformation the Hooke's law must be valid.
(3) Shear stress is equal to zero. The influence about friction is not speculated.
(4) Projected areas are equal.

Point Contact

Two spherical bodies are contiguous in only one point. Owing to load and deformation of the bodies the point contact varies into surface contact (Figure 2). This surface is elliptic. When the bodies are geometrical identical, the contact surface is circular (Herák 2005; Zachariáš 2005).

The maximum sizes of an ellipse the main radiuses are in the main geometrical directions of the contact surface. For calculation Hertz replaced this ellipse by a circle of the same surface (Hertz 1896). Then he derived the equation for the diameter of the contact surface δ (Timoshenko & Goodier 1951)

$$\delta = 2\,m\,\sqrt[3]{\frac{3\,F}{E_R\,\rho_H}} \qquad (3)$$

where:
F – load force,
m – coefficient which characterizes the pressure distribution between bodies. The m value is calculated using
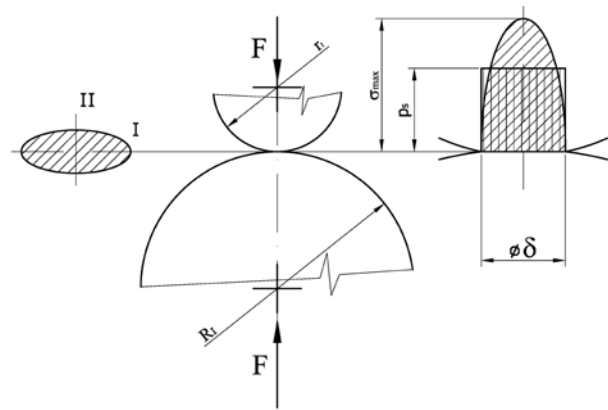

Figure 2. Diagram of the point contact

the solution of elliptic integrals. The coefficient m can be found in form of a table in the literature (Fröhlich 1980).

ρ_H – the sum of the surfaces curvature radiuses.

$$\rho_H = \frac{1}{r_I} \pm \frac{1}{r_{II}} + \frac{1}{R_I} \pm \frac{1}{R_{II}} \qquad (4)$$

where:
$r_I,\ r_{II},\ R_I,\ R_{II}$ – curvature radiuses of single bodies in the directions of main planes.
  In the case of the concave contact they are added (+), in the case of the convex contact they are subtracted (Figure 3).
E_{12} – theoretical reduced modulus of elasticity in tension of the contact bodies.

$$\frac{1}{E_{12}} = \left(\frac{1}{E_{1o}} + \frac{1}{E_{2o}} \right) \frac{1}{2} \qquad (5)$$

$E_{1o},\ E_{2o}$ – constrained modulus of elasticity in tension (the bodies cannot arbitraily deform, their deformations interact)

$$E_{1o} = \frac{E_1}{1-\mu_1^2}, \qquad E_{2o} = \frac{E_2}{1-\mu_2^2} \qquad (6)$$

where:
E_1, E_2 – modulus of elasticity in tension of single bodies,
μ_1, μ_2 – Poisson's ratio of single body materials.
E_R – reduced modulus of elasticity in tension:
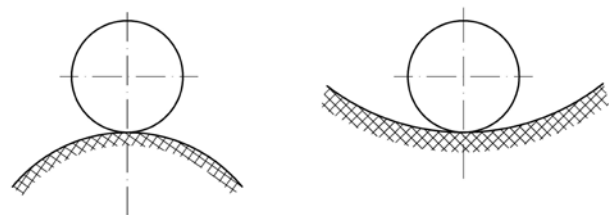

Figure 3. Concave (+) and convex (–) contact of the bodies

Table 1. Material of contact couples and its reduced modulus of elasticity in tension

Material of contact couples	Reduced modulus of elasticity in tension E_R (MPa)
Steel + steel	226 000
Steel + bronze	152 500
Steel + gray iron	121 500

$$E_R = \sqrt[3]{\varphi_E}\, E_{12} \tag{7}$$

where:

φ_E – constant which expresses the material influence of bodies which contact.

For steel/steel $\varphi_E = 1$ for other materials combination the values are shown in Table 1 (Fröhlich 1980).

After introducing in former equations we can determine the reduced modulus elasticity in tension for most often used contact couples.

When we know the diameter value of the contact surfaces δ we can simply determine the surface stress p_s (we presuppose the even, rectangular pressure distribution) (Figure 4).

$$p_s = \frac{F}{S} = \frac{F}{\dfrac{\pi \delta^2}{4}} \tag{8}$$

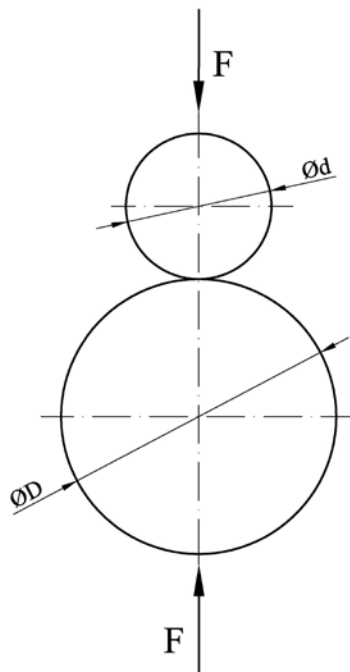But the real contact stress distribution is parabolic. For the point contact the ratio between the

Figure 4. Contact of two spheres

average contact stress and maximum contact stress (Hertz 1896; Timoshenko & Goodier 1951)

$$\sigma_{max} = 1.5 \times p_S \tag{9}$$

After simple introduction we can write the equation

$$\sigma_{max} = 1.5 \frac{4F}{\pi \delta^2} \tag{10}$$

After the equation adaptation, simplification and introduction in former equation we can write the equation for the maximum contact pressure at the point contact.

$$\sigma_{max} = 1.5 \cdot \frac{F}{\pi \left(2\sqrt[3]{\dfrac{3F}{E_R \rho_H}} \right)^2} \tag{11}$$

The maximum contact stress value depends on the load, material of contact bodies, bodies geometry and contact type (concave, convex).

For different geometry of any bodies the calculation can be made using the former equations, but for calculation the bodies must be substituted by osculating circles and the cage solved as the point contact of two spheres.

Contact stress – contact of two spheres

We describe the calculation of contact stress of two spheres, for calculation we choose the steel of body materials. For other materials the calculation is the same, only the material constants are others.

From former chapter we know the reduced modulus of elasticity of the contact bodies (steel + steel): $E_R = 226\,000$ MPa

The sum of main planes flexion radiuses we determine according to the equation

$$\rho_H = \frac{1}{r} \pm \frac{1}{R} + \frac{1}{r} \pm \frac{1}{R} = 4\frac{1 \pm \dfrac{d}{D}}{d} \tag{12}$$

When we introduce the former equation in the equation (3), we get the equation for the contact surface diameter.

$$\delta = 2\,m\sqrt[3]{\frac{3F}{E_R \rho_H}} = 2 \times 0.45 \sqrt[3]{\frac{3F}{226\,000 \; 4\dfrac{1 \pm \dfrac{d}{D}}{d}}} \tag{13}$$

The mean coefficient m for the contact of two spheres steel/steel is approximately equal to

$m = 0.45$. The value depends on the flexion and the total geometry of the bodies (FRÖHLICH 1980). By simple adaptation we get the equation for the diameter of the deformed surface.

$$\delta = 29.8 \sqrt[3]{\dfrac{F}{\left(1 \pm \dfrac{d}{D}\right)} d} \qquad (14)$$

The symbol +/– determines the concave and convex contact.

After introduction in the relation (11) the equation derived by us for the contact surface diameter we get the relation for the maximum contact stress value of two steel spheres

$$\sigma_{max} = 1.5 \dfrac{4F}{\pi \delta^2} = 1.5 \dfrac{4F}{\pi \left(0.0298 \sqrt[3]{\dfrac{F}{\left(1 \pm \dfrac{d}{D}\right)} d} \right)^2} \qquad (15)$$

after a simple adaptation we get

$$\sigma_{max} = 2150 \sqrt[3]{\dfrac{F}{d^2} \left(1 \pm \dfrac{d}{D}\right)^2} \qquad (16)$$

Line contact

It is a contact of two cylindrical bodies, the theoretical contact line is deformed by load into a tetrahedral concurrent surface.

In practice the contact stress is calculated by use of substituted contact cylinders, both cylindrical bodies are substituted by cylindrical bodies with reduced radiuses.
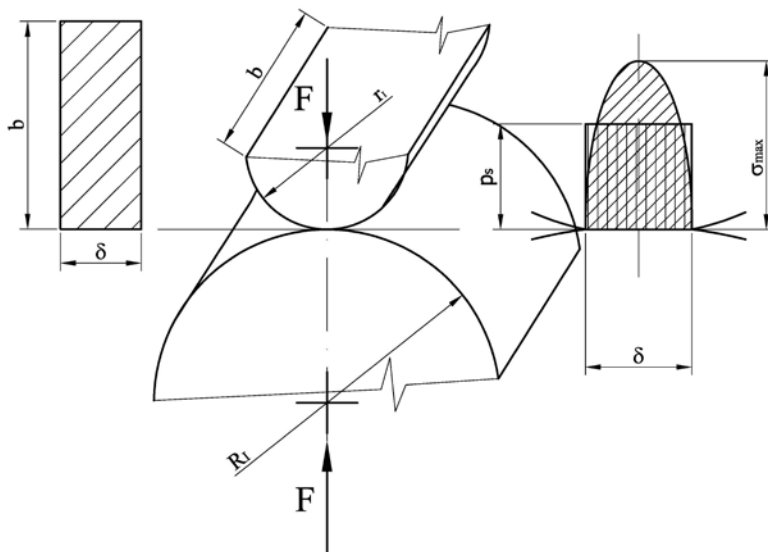
Contact cylinder with cylinder

At the contact of two cylinders the contact line grows in the tetrahedral form.

For the contact surface calculation Hertz derived following relation (HERTZ 1896; TIMOSHENKO & GOODIER 1951).

$$\delta = 2 \sqrt{\dfrac{8}{\pi} \times \dfrac{F}{b \times E_R \times \rho_H}} \qquad (17)$$

All quantities are the same as at the point contact calculation, in addition the length of the contact line b appears.

If we know the contact surface diameter, we can simply determine the mean surface pressure p_s (we presume the contact distribution uniform, tetrahedral) (Figure 5) (ŠVEC 1999).

$$p_s = \dfrac{F}{S} = \dfrac{F}{\delta b} \qquad (18)$$

But the real course of contact pressure is parabolic. For the point contact the ratio between the mean surface pressure and the maximum contact stress was determined.

Control of Food Quality and Food Research. $= 1.28 \, p_s$ (19)

After simply introduction we can write the equation

$$\sigma_{max} = 1.28 \dfrac{F}{\delta \times b} \qquad (20)$$

By adaptation, simplification and introduction in the former equation we can write the equation for the maximum contact pressure quantity at the line contact.

Figure 5. Diagram of two cylinders contact

$$\sigma_{max} = 1.28 \frac{F}{b \times 2 \sqrt{\dfrac{8}{\pi} \times \dfrac{F}{b \times E_R \times \rho_H}}} \qquad (21)$$

Further we describe the calculation of the contact stress at two cylinders contact. The cylinder material is steel. For other materials the calculation is the same, only the material constants are different.

From the chapter 4 we know the reduced modulus of elasticity of the contact bodies (steel + steel):
E_R = 226 000 MPa

The sum of main planes flexion radiuses we determine according to the equation.

$$\rho_H = \frac{1}{r} \pm \frac{1}{R} = 2 \frac{1 \pm \dfrac{d}{D}}{d} \qquad (22)$$

When we introduce the equation (22) in the equation (17), we get the equation for the contact plane width calculation.

$$\delta = 2 \sqrt{\frac{8}{\pi} \times \frac{F}{b \pm E_R \times \rho_H}} = 2 \sqrt{\frac{8}{\pi} \times \frac{F}{b \times 226\,000 \times 2 \times \dfrac{1 \pm \dfrac{d}{D}}{d}}} \qquad (23)$$

After a simple adaptation we get the equation for the contact plane width calculation.

$$\delta = 4.74 \sqrt{\frac{F \times d}{b \left(1 \pm \dfrac{d}{D}\right)}} \qquad (24)$$

The symbol +/− determines the concave and convexe contact.

When we introduce the equation (24) derived by us into the equation (21) we get the relation of the maximum contact tress at the two steel cylinder contact.

$$\sigma_{max} = 1.28 \frac{F}{b \times 4.74 \times 10^{-3} \sqrt{\dfrac{Fd}{b \left(1 \pm \dfrac{d}{D}\right)}}} \qquad (25)$$

After a simple adaptation we get

$$\sigma_{max} = 270 \sqrt{\frac{F}{b \times d} \left(1 \pm \frac{d}{D}\right)} \qquad (26)$$

Contact pressures cone-cone

At the calculation of cone-cone contact pressure the two-dimensional line contact originates. The calculation is the same as at the contact cylinder-cylinder, but the initial equation (26) is multiplied by a constant of the contact pressure K resultant position. This constant is described by several authors in special literature (Fröhlich 1980) presents the value K = 0.33.

Further this constant is described by e.g. Berndt, Bochman, Föppel, Palmgren, Lundberg, Klaptrod, Faires and others.

Equations derived by formerly mentioned authors are mostly functions determined from complete elliptic integrals (Tripp 1985). Using these integral formulas the constant result is approximately K = 0.3.

In practice the calculation according to Fröhlich is suitable.

$$\sigma_{max} = 270\,K \sqrt{\frac{F}{l \times d} \left(1 \pm \frac{d}{D}\right)} = 270 \times 0.33 \sqrt{\frac{F}{l \times d} \left(1 \pm \frac{d}{D}\right)} = 89.1 \sqrt{\frac{F}{l \times d} \left(1 \pm \frac{d}{D}\right)} \qquad (27)$$

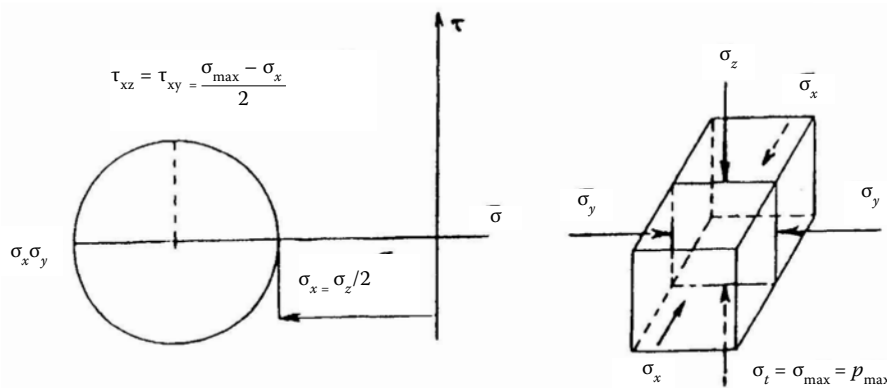When we express the force F we get the formula (27).

Figure 6. Pressure stress acting on the elementary joist placed in the middle of the contact length b

$$F = \left(\frac{\sigma_{max}}{89.1}\right)^2 \frac{l \times d}{\left(1 \pm \dfrac{d}{D}\right)} = \left(\sigma_{max}\right)^2 \frac{1}{7938.81} \times$$

(28)

$$\times \frac{l \cdot d}{\left(1 \pm \dfrac{d}{D}\right)} = 27\frac{l \times d}{E}\left(\frac{\sigma_{max}}{\Delta}\right)^2$$

where:

$$\Delta = \sqrt{1 \pm \frac{d}{D}} \ .$$

When we express the force F from the former formula, we get the equation for the maximum contact force at the contact cone-cone.

$$F = 27.7\frac{l \times d}{E}\left(\frac{\sigma_{max}}{\Delta}\right)^2$$

(29)

Pitting

In the former chapter we derived the equations for the contact surface size and for the course of contact pressures distribution. From practical stress measurements of two cylindrical bodies contact the course of stress distribution in the body sections near the contact surface was determined. If we shall speculate about the bodies relative motion (what is the typical example of the friction drive), except the contact pressure the very high friction force will act in the contact surface (Krause & Demirci 1975).

In the contact place in the middle of the contact length b three normal pressure stresses σ_y, σ_x, σ_z act on the elementary joist. The stress σ_y and σ_z are equal $\sigma_y = \sigma_z = \rho_{max}$, while in the x direction the pressure stress is only half $\sigma_x = 0.5\rho_{max}$ (Figure 6). When we plot these stresses in the Mohr's circle, we get the

overview about the stress distribution in the given element sections (Figure 6). It is evident that the maximum shear stress in the middle of the contact surface is in the planes which are diverted from the axis y or if need be z direction of an angle $\gamma = 4.5°$ and its value is $\tau_{xz} = \tau_{xy} = 0.5 (p_{max} - \sigma_x)$

If we effect the section through the body in the plane parallel with the contact surface in a low depth under the contact surface, the normal stresses will be according to the increase of the section plane minor and of course different (Figure 7) from the state stress. The representation using Mohr's circles for triaxial state of stress gives us again the graphic view of the stress distribution in the element (Figure 8) (Faires 1955; Krause & Jühe 1977).

If we plot single normal stresses in the sections parallel to the contact surface in various distance from the contact surface we get the graphically relation between the stress and the depth of cut (Figure 7). From here derived shear stresses $\tau_{yz} = (\sigma_z - \sigma_y)/2$, $\tau_{xz} = (\sigma_z - \sigma_x)/2$, $\tau_{xy} = (\sigma_y - \sigma_x)/2$, which act in the planes diverted of 45° from the planes given by the axes yz, xz, xy are graphically presented in Figure 8.

From the shear stresses distribution can be seen that the maximum shear stress value τ_{yz} appears in the depth of cut near to $(0.35-0.40)b$. If we combine vectorial the shear stress τ_{yz} and the shear stress τ_s which is needed for the shear friction force blocking in the contact surface, we get very high resulting shear stresses in the planes α and β, which are diverted from the plane given by the directions xy of the angle κ (Figure 8).

Material crystals near the middle of the contact surface are largely stressed by volume compression, which evokes their partial plastic deformation. In
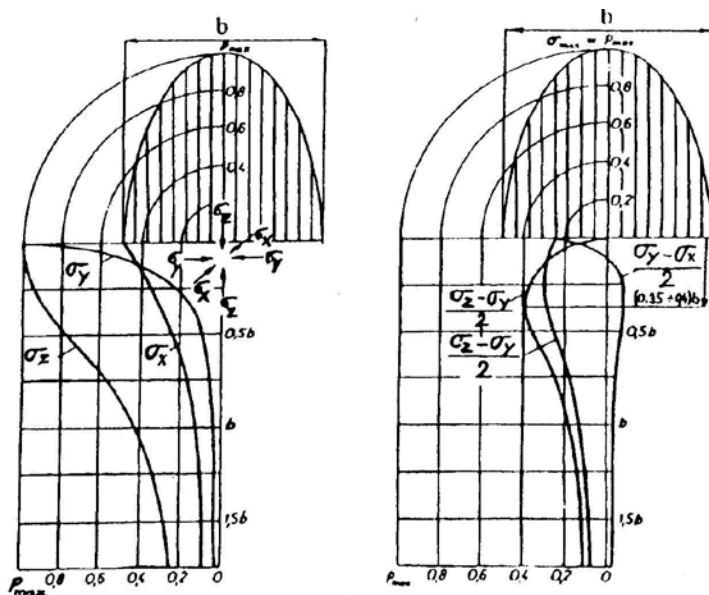

Figure 7. Stress distribution on elementary joists in the z – axis section in the depth 1.5b under the contact surface

$$\tau_{xy} = \frac{(\sigma_y - \sigma_x)}{2}$$
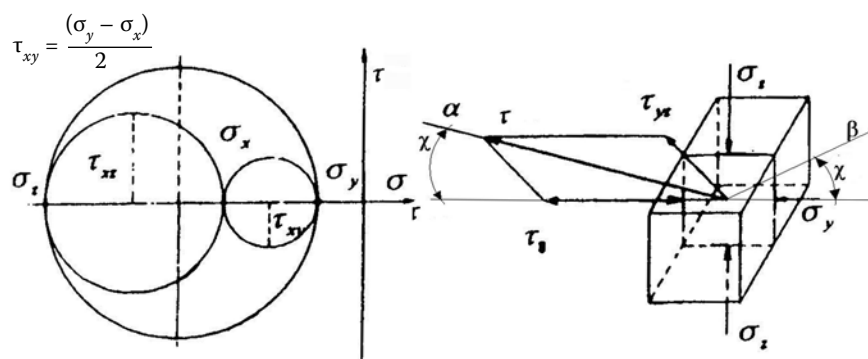
Figure 8. Stress distribution in the section parallel to the contact surface in the depth of 0.35b under the contact surface

the limiting depth of about 0.35 *b* the influence of the high resultant shear stress begins to predominate, so that near the contact surface the complex of pressed crystals can be cut off from the cylinder surface under the angle *κ* (Figure 8). The whole effect of excessive compression of the crystal complex and their subsequent cut off from the surface is called as pitting (Král 2002).

CONCLUSIONS

The operation of friction drives is influenced by a great number of operating factors. Bearing stress, slippage, heating-up and wear.

Factors which influence the bearing stress are following: friction bodies' material, contact stress, contact bodies moving, medium of the contact process and the general environs of the contact.

The fact that these factors affect one another (slippage against temperature, temperature against material etc.) shows the whole problem complex of the friction origin and thus the origin of contact stresses in friction drives.

It is very clear from the variety of affected factors that the friction force or contact pressures value cannot be calculated according to simple basic equations and rules (Krause & Demirci 1975).

For the bearing stress i.e. contact pressures value calculation the Hertz's equations are used. Heinrich Hertz derived the basic equations which depend on the input coefficients, which depend on the sizes and dimensions of contact bodies. In next years these coefficients were presented by various authors either using the tables of dimensional coefficients (Fröhlich 1980) or using the calculation of total elliptic integrals (Tripp 1985). During the time various equations have come into being which were derived from the combination of the basic Hertz's and the empirical equations.

The relations determined in this paper are derived more simply, but in our opinion they are suitable for usual machine industry and applications in friction drives.

In design practice the contact stresses calculation is always the combination of theoretical Hertz's equations and coefficients or empirical relations, which were determined and tested by a long-standing operation of machines. E.g. for the calculation of contact stress of two teeth of involutes gearing a very detailed elaborated design procedure exists, which is long-termed tested and gives very accurate results (Švec 1999; Král 2002; Bolek & Kochman 1989).

If we do not take into account the influence of real factors which affect the contact stressed value the calculated contact stress can be different from real stress up to 50% (Klapdtrot 1980). Namely the Hertz's equations for contact stress are derived from *3D* analysis, but most of input information for these equations are determined using the *2D* analysis. Next disadvantage of these equations is the fact that they do not respect the contact surfaces roughness and the premise that the stress peaks point at the middle of contact surfaces (Jagodnik & Müftü 2003).

At friction drives the influence of contact bodies moving exists, too. From the basic condition of the friction drive it follows that in the contact surface except the contact pressure a very high friction force acts (Krause & Jühe 1977).

On the basis of Hertz's equations the equations and methods for calculation of unelastic contact of two bodies were determined. The equations of contact state at unelastic contact speculate about energy lost at reciprocal deformation of two bodies (Gugan 2000).

Today the procedures and methods of contact pressures calculation of nonmetallic bodies (glass, granite) and at contact in different medium (water, oil, etc.) exist, too. These equations were again derived using the original Heinrich Hertz's theory (Franco & Batzoglou 2002).

On the basis of theoretical Hertz's equations for contact pressures calculation a great number of calculation and application techniques exist. They are determined for various branches of science, from biomedicine, e.g. calculation of contact pres-

sures at hip joints, contact pressures between track and wheel at rail transport, in terramechanic, i.e. analysis of tyre contact with soil, tribology – calculation of lubricating layer load capacity to the known engineering applications, e.g. calculation of bearings and gear wheels.

By its theoretical equations Heinrich Hertz makes possible the development of more detailed and exact calculation and analyses of single design problems. On basic of its theories the new modern methods continuous arise from various branches of human research. These analyses are derived only analytically using empirical data and serve as the basis for the problems solution on the FEM basis.

References

Bolek A., Kochman J. (1989): Části strojů, svazek 1. SNTL, Praha.

Bolek A., Kochman J. (1990): Části strojů, svazek 2. SNTL, Praha.

Faires V.M. (1955): Design of Machine Elements. The Macmillan Company, New York.

Franco G.E., Batzoglou A.C. (2002): An elastic contact mechanics fracture flow model. In: 15th ASCE Engineering Mechanics Conf., Columbia University, New York.

Fröhlich J. (1980): Technika uložení s valivými ložisky. SNTL, Praha.

Gugan D. (2000): Inelastic collision and the Hertz theory of impact. American Journal of Physics Teachers, **68**: 8.

Herák D. (2005): Mechanické variátory otáček pro přenášený výkon 0 až 50 kW. [Doktorská dizertace.] TF ČZU, Praha.

Hertz H. (1896): Miscellaneous Papers. Macmillan and Co.,New York.

Jagodnik J.J., Müftü S. (2003): A cylindrical contact model for two dimensional multiasperity profiles. In: Proc. STLE/ASME Int. Joint Tribology Conf., Ponte Vedra Beach, Florida.

Klaprodt T. (1980): Untersuchungen zur statischen Tragfähigkeit gehärteter Stahloberflächen bei Hertz'scher Pressung. UH FfM, Hannover.

Král Š. (2002): Části a mechanizmy strojov. II. Diel. STU, Bratislava.

Krause H., Demirci A.H. (1975): Factors influencing the real trend of the coefficient of friction of two elastic bodies rolling over each other in the presence of dry friction. In: Proc. Symp. Int. Union of Theoretical and Applied Mechanics, Delft University Press, Netherlands, 342–357

Krause H., Jühe H.H. (1977): Internal stresses during rolling friction and their evaluation. Wear 41, Elsevier Sequoia S.A., Lausanne – printed in the Netherlands, 15–23.

Švec V. (1999): Části a mechanismy strojů – Mechanické převody. ČVUT, Praha.

Timoshenko S.P., Goodier J.N. (1951): Theory of Elasticity. Mc Graw-Hill, New York.

Tripp J.H. (1985): Hertzian Contact in Two and Three Dimensions. Nasa Technical Paper 2473, Lewis Research, Cleveland, Ohio.

Zachariáš L. (2005): Části strojů. ČZU, Praha.

Abstrakt

Herák D., Chotěborský R., Sedláček A., Janča E. (2006): **Využití Hertzových kontaktních tlaků v třecích převodech.** Res. Agr. Eng., **52**: 107–114.

Článek je zaměřen na aplikace rovnic popisujících velikosti Hertzových kontaktních tlaků vznikajících v třecích převodech. V článku jsou odvozeny zjednodušené rovnice vhodné pro výpočet kontaktních napětí vznikajících v třecích převodech při styku koule – koule, válec – válec, kužel – kužel a jejich grafické znázornění rozložení napětí v kontaktní plošce. Pomocí Hertzových kontaktních tlaků a aplikací Mohrových kružnic je v článku odvozena podstata vzniku pittingu a jsou zobrazeny průběhy napětí na elementárních hranolcích, ležících na ose z v řezech vedených pod kontaktní ploškou.

Klíčová slova: kontaktní tlaky; třecí převod; Hertzovy tlaky; pitting; třecí síla; Mohrovy kružnice

Corresponding author:

Ing. David Herák, Ph.D., Česká zemědělská univerzita v Praze, Technická fakulta, katedra mechaniky a strojnictví, Kamýcká 129, 165 21 Praha 6-Suchdol, Česká republika
tel.: + 420 224 383 186, fax: + 420 220 921 361, e mail: herak@tf.czu.cz